

Highly Hydrophilic Fused Aggregates (Microsponges) from a C12 Spermine Bolaamphiphile

Pei Lee Kan,[†] Brigitte Papahadjopoulos-Sternberg,[§] Dennis Wong,[†] Roger D. Waigh,[†] Dave G. Watson,[†] Alexander I. Gray,[†] Dave McCarthy,^{||} Mark McAllister,⁺ Andreas G. Schätzlein,[‡] and Ijeoma F. Uchegbu^{*,†}

Department of Pharmaceutical Sciences, University of Strathclyde, 27 Taylor Street, Glasgow G4 0NR, U.K., Cancer Research U.K., Department of Medical Oncology, University of Glasgow, Garscube Estate, Glasgow G61 1BD, U.K., NanoAnalytical Laboratories, San Francisco, California 94118, Electron Microscopy Unit, School of Pharmacy, University of London, 29-39 Brunswick Square, London WC1N 1AX, U.K., GlaxoSmithKline, New Frontiers Science Park (South), Third Avenue, Harlow, Essex, CM19 5AW, U.K.

Received: October 24, 2003; In Final Form: March 23, 2004

Bolaamphiphiles consist of two hydrophilic headgroups joined by a hydrophobic linker. They are known to self-assemble into vesicles, micelles, tubules and fibers. Here we report on the self-assembly of a 1,12-[*N,N*-bis(3-aminopropyl)-1,4-butane diamine] dodecane (12G1) in aqueous media into discrete nonbilayer nanoparticles and unusual fused highly hydrated sponge like structures. 12G1, 1,10-[*N,N*-bis(3-aminopropyl)-1,4-butane diamine] decane (10G1), 1,8-[*N,N*-bis(3-aminopropyl)-1,4-butane diamine] octane (8G1), and 1-[*N,N*-bis(3-aminopropyl)-1,4-butane diamine] dodecane (12G0) were synthesized and their self-assembly studied. 12G0 was relatively insoluble in water and multilamellar vesicles were produced with this amphiphile and cholesterol. While no aggregation in aqueous media was recorded for either 10G1 or 8G1 up to a concentration of 20 mM, aggregation of 12G1 molecules was seen to take place at an aqueous concentration of 1.75 mM as determined using various fluorescent and colorimetric probes and surface tension measurements. Electron microscopy images revealed that 12G1 formed monolayer vesicles of 20 nm in size at a concentration of 2.6 mM and even larger fused aggregates when the concentration was increased to 35 mM. Fusion resulted from the bridging of vesicles by the bolaamphiphile molecules. 12G1 aggregates encapsulated 23X more low molecular weight (4kD) FITC-dextran than high (250kD) molecular weight FITC-dextran, an indication of the limited volume of the hydrophilic domains. 12G1 also encapsulated 137X more 4kD FITC-dextran than was encapsulated by conventional sorbitan monostearate vesicles. We conclude that highly hydrated aggregates consisting of fused monolayer vesicles with small discrete hydrophilic domains in a sponge like structure may be formed by the self-assembly of bolaamphiphiles.

Introduction

Bolaamphiphiles are compounds in which a hydrophobic spacer bridges two hydrophilic moieties (Figure 1), and their self-assembly has been studied since the 1980s.¹ Vesicles and micelles are usually reported¹ and result from hydrophobic interactions of the hydrophobic spacer groups. However, occasionally there have been reports of tubules^{2,3} and nanofibers⁴ which result from further hydrogen bonding associations of the molecules along the tubular axis in addition to the aforementioned hydrophobic associations. While a detailed structure activity relationship study of bolaamphiphiles and their resulting assemblies has not been carried out, data generated suggest that the spherical self-assemblies of bolaamphiphiles may be classified according to the length of the hydrophobic spacer unit within a given structural class. Long-chain bolaamphiphiles, containing a hydrophobic spacer (>C16), form both micelles⁵ and monolayer (membrane spanning amphiphile) vesicles,⁶ and

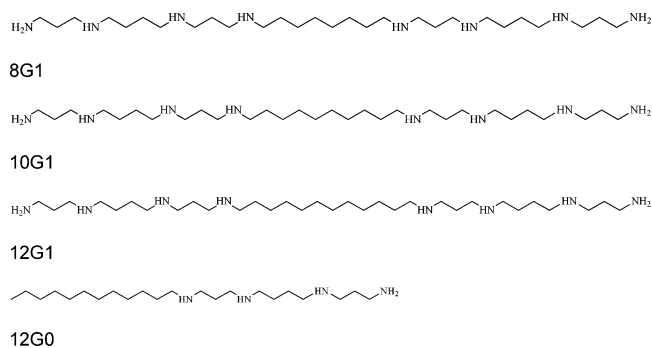


Figure 1. Spermine amphiphiles.

while monolayer vesicles are formed from double short-chain C12 bolaamphiphiles^{1,7} in aqueous media, single-chained bolaamphiphiles possessing a short hydrophobic spacer (C8 or C12) (termed short chain bolaamphiphiles here) have only been shown to form vesicles when possessing a planar (urocanic acid — comprising an imidazole unit) headgroup.⁵ Other short chain bolaamphiphiles have been described as forming various spherical aggregates of unspecified architecture^{8–10} Also, apart from the C12 asymmetric ω -hydroxy quaternary ammonium surfactants,¹¹ micelles have rarely been reported with short single-

* Corresponding author. Fax: +44 141 552 6443. E-mail: i.f.uchegbu@strath.ac.uk.

[†] University of Strathclyde.

[‡] University of Glasgow.

[§] NanoAnalytical Laboratories.

^{||} University of London.

⁺ GlaxoSmithKline.

chain bolaamphiphiles. The difficulty for short chain bolaamphiphiles to adopt a U-shaped conformation except under certain conditions where there is stabilization of the headgroups in such a conformation¹² has been cited as a reason for this latter observation.¹³ We are interested in the supramolecular assemblies that may be formed from these short chain amphiphiles as an understanding of the self-assemblies formed from short chain bolaamphiphiles could provide an insight into the fundamental variables governing self-assembly, especially as in some cases no supramolecular structures are detected with short chain bolaamphiphiles.^{14–16} Hence a study of the short chain species will provide details on the minimum hydrophobic chain length that is necessary for the formation of various aggregates and may even as reported here lead to the discovery of new self-assembled structures. Here we report on the self-assembly of a C12 spermine bolaamphiphile (Figure 1) into novel highly hydrated sponge like aggregates in which extremely small vesicles are fused by the bridging of these double headed surfactants. Our studies demonstrate that the C12 spacer is the minimum spacer length which supports such aggregates and also that bolaamphiphiles are capable of facilitating vesicular fusion to form multivesicular structures which have not been reported previously.

Materials

Spermine, 1,8-dibromooctane, 1,10-dibromodecane, 1,12-dibromododecane, dodecyl bromide, pyrene, 2-p-toluidinylnaphthalene-6-sulfonic acid (TNS), 1,6-diphenyl-1,3,5-hexatriene, methyl orange, polysorbate 20, sorbitan monostearate, sodium bicarbonate, and 200 nm polystyrene beads were all obtained from Sigma Aldrich Co., U.K. All solvents were purchased from the Department of Pure and Applied Chemistry, University of Strathclyde, U.K. Visking tubing was obtained from Medicell International, U.K. Distilled water was obtained from a doubly distilled source (Aquatron A4D, Bibby Sterilin, U.K.).

Methods

Synthesis. *8G1.* To spermine (1 g) dissolved in absolute alcohol was added sodium bicarbonate (2 g). To this mixture was added dropwise with stirring over a 2 h period 1,8-dibromododecane (0.33 g) dissolved in absolute alcohol (100 mL). The reaction mixture was stirred and refluxed for 4 h, after which the resulting precipitate was removed by filtration and the filtrate evaporated to dryness under reduced pressure at 70 °C. The white residue from above was added to propan-2-ol (100 mL) and left overnight. The propan-2-ol was removed by centrifugation (10 000 rpm \times 10 min, Hermle Z323K, LaborTechnik, Germany) at 10 °C and the pelleted product left to air-dry. The air-dried product was subsequently dissolved in distilled water (100 mL) and freeze-dried. The product was recovered as a white solid.

10G1. To spermine (1 g) dissolved in absolute alcohol was added sodium bicarbonate (2 g). To this mixture was added dropwise with stirring over a 2 h period 1,10-dibromododecane (0.36 g) dissolved in absolute alcohol (100 mL). The reaction mixture was stirred and refluxed for 4 h and the product isolated as outlined for 8G1.

12G1. To spermine (2 g) dissolved in absolute alcohol (10 mL) was added sodium bicarbonate (1.7 g). To this mixture was added dropwise with stirring over a 1 h period 1,12-dibromododecane (0.32 g) dissolved in absolute alcohol (60 mL). The reaction mixture was stirred and refluxed for 4 h, after which the precipitate was filtered off. The filtrate was evaporated to dryness under reduced pressure at 70 °C and the

resulting white residue dissolved in distilled water (30 mL) and subjected to exhaustive dialysis (Visking seamless cellulose tubing, molecular weight cutoff 12–14 kD) against distilled water (5 L with 6 changes over a 24 h period). The product was then freeze-dried and recovered as a white solid.

1-[N,N-Bis(3-aminopropyl)-1,4-butane diamine]dodecane (12G0). To spermine (5 g) dissolved in absolute ethanol (15 mL) was added sodium bicarbonate (4 g). To the mixture was subsequently added dropwise and with stirring 1-bromododecane (0.65 mL) dissolved in absolute ethanol (150 mL). The reaction mixture was refluxed with stirring for 4 h. The filtrate was isolated and the ethanol evaporated to dryness by rotary evaporation under reduced pressure at 70 °C. The residue was mixed with distilled water (20 mL) and exhaustively dialyzed as detailed above. Once again the product was isolated by freeze-drying.

¹H NMR. ¹H NMR, ¹³C NMR, and ¹H correlation experiments were performed on all products dissolved in CD₃OD on a Bruker AMX 400 MHz NMR spectrometer.

Electrospray Ionization Mass Spectroscopy. Electrospray ionization mass spectroscopy was performed on all products. Samples were dissolved in a mixture of methanol, 0.1% w/v formic acid (1:1) and analyzed (Automass Multi GC/LC-MS, Thermoseparations, U.K.). The instrument was operated in the positive ion electrospray mode with a source temperature of 250 °C and a cone voltage of 22 V.

Aggregation in Aqueous Media. *Pyrene Probe.* A solution of pyrene (2 μ M) was prepared by dissolving pyrene (40 mg) in absolute alcohol (100 mL). A 100 μ L sample of this solution was placed in a 100 mL volumetric flask and the ethanol evaporated off under a stream of nitrogen gas. The flask was made up and the emission spectra of the pyrene solution recorded (340–600 nm) at an excitation wavelength of 335 nm (Perkin-Elmer LS50B fluorescence spectrophotometer, Perkin-Elmer Instruments, U.K.). The fluorescence spectra of various 12G1 dispersions in the pyrene solution were also recorded as described above. 12G1 dispersions were obtained by probe sonication (as described above). From the pyrene emission spectra, the ratio of the intensity of the third to the first vibronic peaks (I1/I3)¹⁷ were recorded.

Methyl Orange Probe. Various concentrations of 8G1, 10G1, and 12G1 were dispersed by probe sonication in a solution of methyl orange (25 μ M) in borate buffer (0.02 M, pH 9.4). Dispersions were incubated for 1 h at 25 °C and their UV absorption spectra recorded (350–600 nm).¹⁸ The absorption spectra of the aqueous methyl orange solution served as a control.

1,6-Diphenyl-1,3,5-hexatriene. A methanolic solution of 1,6-diphenyl-1,3,5-hexatriene (0.4 mM, 10 μ L) was added to various concentrations of 12G1 (1 mL) and the samples stored in the dark for 2 h. The UV absorbance (356 nm) of these dispersions were then recorded.¹⁹ The absorbance of a control solution, prepared by adding 1,6-diphenyl-1,3,5-hexatriene (0.4 mM, 10 μ L) to water (1 mL), was also recorded. This latter solution served as a reference solution during measurements.

Surface Tension Measurements. Surface tension measurements were made at 20 °C on 12G1 dispersions using the Wilhelmy plate technique (Torsion Balance, Sarose Scientific Instruments, U.K.) with a microscope glass coverslip (2.4 cm \times 2.4 cm).

¹H NMR Studies in D₂O. ¹H NMR scans were performed on dispersions of 12G1, 12G0, polysorbate 20, and sorbitan monostearate in D₂O. Samples were run on a Bruker AMX 400MHz NMR spectrometer.

Imaging of Aggregates. Freeze-Fracture Transmission Electron Microscopy. The sample was cooled using the sandwich technique and liquid nitrogen-cooled propane. Using this technique a cooling rate of 10 000 K/s is reached avoiding ice crystal formation and any artifacts arising from the cryofixation process. The fracturing process was carried out in JEOL JED-9000 freeze etching equipment and the exposed fracture planes were shadowed with platinum for 30 s at an angle of 25–35° and subsequently with carbon for 35 s (2.5 kV/60–70 mA, 1×10^{-5} Torr). The resulting replicas were cleaned with concentrated, fuming nitric acid for 24–36 h followed by repeated agitation with fresh chloroform, methanol (1:1) for at least 5 washes. The carefully cleaned replicas were imaged with a JEOL 100 CX electron microscope.

Nanoviscosity of Hydrophobic Domains. 2-*p*-Toluidinyl-naphthalene-6-sulfonic Acid (TNS) Assay. To 10 mL volumetric flasks, was added TNS (0.5 mL, 100 μ M) dissolved in water. To the flasks were added 1 mL aliquots of various concentrations of either 12G1 aggregates, sorbitan monostearate, and cholesterol (1:1) vesicles in water and the volume made up with water. The 12G1 and the sorbitan monostearate formulations were dispersed by probe sonication. The stoppered dispersions were subsequently equilibrated by shaking for 10–15 s. Fluorescence emission spectra were recorded for various concentrations of the amphiphiles (excitation wavelength = 323 nm). The wavelength of maximum fluorescence of all the samples was recorded as a measure of the polarity/viscosity of the probe environment.²⁰

Analysis of Hydrophilic Domains. Entrapment of FITC-Dextran in 12G1 Aggregates. 12G1 (14 mM, 8 mg mL⁻¹) was sonicated in the presence of fluorescein isothiocyanate–dextran (FITC-dextran, 1% w/v) of various molecular weights (4, 10, 20, 70, and 250 kD). The separation of entrapped FITC-dextran from the untrapped material was accomplished by ultracentrifugation (Beckman L8-M Ultracentrifuge, 150 000g for 1 h) of the 2 mL dispersion, followed by isolation of the pellet. To quantify the level of entrapment of FITC-dextran, the entire pellet was disrupted with absolute alcohol (5 mL), the resulting solution diluted 200X with distilled water, and the FITC-dextran quantified fluorimetrically ($\lambda_{\text{excitation}} = 495$ nm, $\lambda_{\text{emission}} = 520$ nm) against a standard curve prepared from aqueous FITC-dextran solutions (0–25 μ g mL⁻¹). The entrapment efficiency of sorbitan monostearate vesicles (8 mg mL⁻¹) and sorbitan monostearate, cholesterol vesicles^{21,22} (8 mg mL⁻¹, 4 mg mL⁻¹) was also determined against a similar concentration of 4 kD FITC-dextran.

Results and Discussion

Synthesis and Characterization of Amphiphiles. The alkylation of spermine by dibromoalkanes yielded a number of spermine based bolaamphiphiles. Dibromoalkanes are known to be good starting materials for the synthesis of bolaamphiphiles.¹

12G1. The yield of 12G1 was 0.9 g. Mass spectrometry data revealed the presence of the mass ion (MW = 570) while NMR data revealed chemical shifts which were assigned as follows: $\delta = 1.23$ (CH₂ – C12 chain), 1.54 (CH₂ – β to one amino group), 1.54 (CH₂ – β to two amino groups), and 2.50–3.00 (CH₂ – α to amino group).

10G1. The yield of 10G1 was 0.5 g. Mass spectrometry data revealed the presence of the mass ion (MW = 543), while NMR data revealed chemical shifts which were assigned as follows: $\delta = 1.30$ (CH₂ – C12 chain), 1.54 (CH₂ – β to one amino group), 1.65 (CH₂ – β to two amino groups), and 2.40–2.65 (CH₂ – α to amino group).

8G1. The yield of 8G1 was 0.3 g. Mass spectrometry data revealed the presence of the mass ion (MW = 515) while NMR data revealed chemical shifts which were assigned as follows: $\delta = 1.30$ (CH₂ – C12 chain), 1.50 (CH₂ – β to one amino group), 1.70 (CH₂ – β to two amino groups), and 2.40–2.60 (CH₂ – α to amino group).

12G0. The yield of 12G0 was 1.2 g. Mass spectrometry data revealed the mass ion (MW = 371) while NMR data revealed chemical shifts which were assigned as follows: $\delta 0.9 = \text{CH}_3$ (dodecane), $\delta 1.3\text{--}1.4 = \text{CH}_2$ (dodecane), $\delta 1.4\text{--}1.8$ ppm = CH₂ (dodecane and spermine groups, β to amino groups), and $\delta 2.4\text{--}2.9$ ppm = CH₂ (α to amino groups).

¹H NMR integration data for 12G1 and 12G0 conformed to the expected structures. 8G1 and 10G1 contained unreacted spermine as an impurity (10–30% w/w), which was difficult to remove. However, this impurity would not interfere with the aggregation of 8G1 and 10G1 as the aggregation of amphiphiles to form colloidal dispersions is known to take place in the presence of water soluble solutes. It should be noted however that actual concentrations of 8G1 and 10G1 were actually 70–90% of that reported using the weighing data.

Aggregation of Amphiphiles in Aqueous Media. Isotropic liquids are formed on dispersion of 8G1 and 10G1 in aqueous media up to a concentration of 20 mM. However, while 12G1 formed isotropic liquids up to a concentration of 10 mM, higher aqueous concentrations of the amphiphile resulted in turbid dispersions, and the particles formed sediment within a few hours.

Figure 2 provides evidence that 12G1 aggregates in aqueous medium. A fall in the I1/I3 ratio in the pyrene emission spectra (Figure 2a) is evidence that the pyrene probe moves from an area of high to low polarity¹⁷ once aggregates are formed and the lowering of the surface tension is evidence of monolayer formation (Figure 2a) prior to aggregation. A minimum surface tension is seen at a concentration of 2.6 mM of the bolaamphiphile (where molecular aggregation is detected with this technique) and a limiting I1/I3 value is seen at a concentration of 1.75 mM, a concentration where there is complete encapsulation of pyrene by the self-assembled molecules. The critical aggregation concentration is thus measured to be 1.75 mM as determined with the pyrene data, which serves as a more sensitive measure of aggregation than the surface tension studies. A sharp inflection in the absorbance versus concentration curve in the case of 1,6-diphenyl-1,3,5-hexatriene²³ (Figure 2b) and a change in the methyl orange wavelength of maximum absorbance (Figure 2b) also indicate a movement of the colorimetric probes from areas of high to areas of low polarity.¹⁸ It is clear that there is no aggregation of either 8G1 and 10G1 at the concentrations studied (Figure 2b). When the surface tension data is analyzed using the Gibbs equation for the adsorption of surfactants (eq 1), the area per molecule (*A*) at the air aqueous interface may be calculated (eq 2)

$$\Gamma_2 = \frac{-1}{xRT} \frac{d\gamma}{2.303 d \log c} \quad (1)$$

where Γ_2 = surface excess concentration calculated from the

$$A = \frac{1}{N_A \Gamma_2} \quad (2)$$

limiting portion of the slope of the surface tension log concentration ($d\gamma/d \log c$) plot, *R* is the gas constant, *x* = 1 for dilute solutions of ionic surfactants, and *T* the temperature in degrees Kelvin. *N_A* = the Avogadro constant. An area per

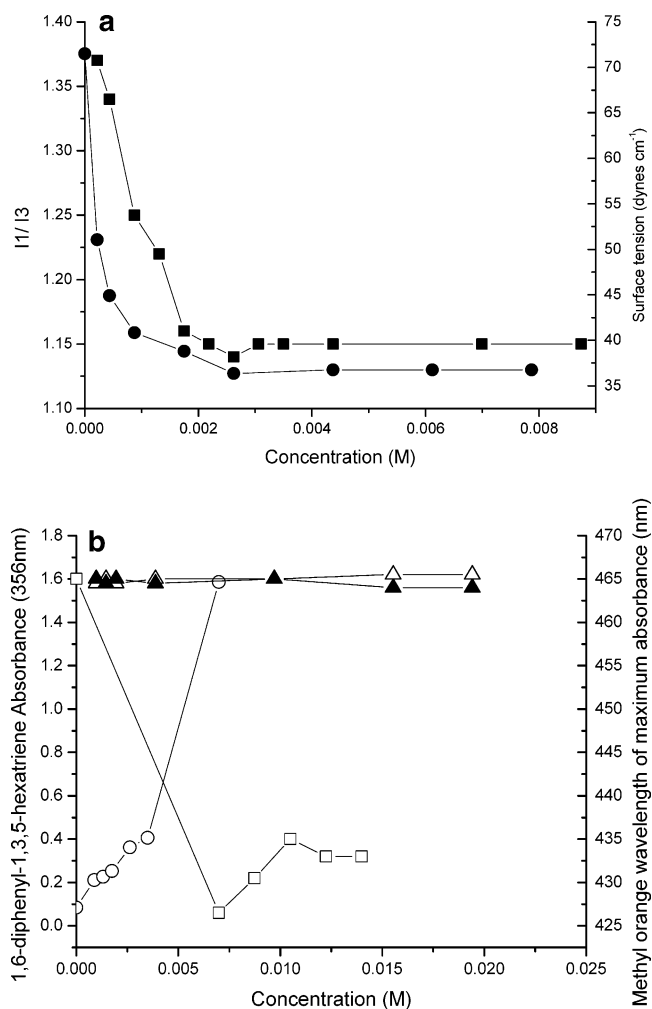


Figure 2. (a) The surface activity (●, right Y-axis) and aggregation (pyrene fluorescence - ■, left Y-axis) of 12G1. A decrease in the I1/I3 ratio is observed once pyrene moves to the hydrophobic environment formed by the aggregating 12G1 molecules. (b) Bolaamphiphile aggregation: (○) = 12G1 1,6-diphenyl-1,3,5-hexatriene data, (□) = 12G1 methyl orange data, (▲) = 10G1 methyl orange data, (△) = 8G1 methyl orange data.

molecule of 73.2\AA^2 is obtained, which suggests that the molecules are lying parallel (with both hydrophilic faces in

contact with the surface) as opposed to perpendicular (with one hydrophilic face in contact with the surface) to the plane of the surface.²⁴ The critical aggregation concentration of 12G1 is 1.75 mM (pyrene data), and the aggregates formed by low concentrations (2.6 mM) of 12G1 are small spherical aggregates of 20–50 nm in size (Figure 3a). Aggregates consist of a few fused spheres (Figure 3a) at lower concentrations (2.5 mM). At higher concentrations (14 mM), 12G1 is seen to form larger fused aggregates (Figure 3b) which sediment in aqueous media. The spherical aggregates formed from 12G1 are non bilayer in nature unlike the 100 nm multilamellar bilayer vesicles formed from the single headed less hydrophilic amphiphile (12G0) with cholesterol (Figure 3c). 12G0 precipitates when dispersed in water at concentrations of 2.7 mM. The 20 nm size of individual 12G1 aggregates suggests that they are also not micelles (polysorbate 20 micelles were sized at about 5–7 nm on our instrumentation), which would have formed if the bolaamphiphile had adopted a U shape. It is unusual to see bolaamphiphiles with a small hydrophobic spacer length (<C10 – C12) aggregating into micelles as micelles are only seen when the spacer length increases to about a C16⁵ due to an inability of small hydrophobic spacer groups to adopt the U-shaped conformation²⁵ except under exceptional circumstances such as where the hydrophilic moieties are anchored together.¹²

¹H NMR data on the 12G1 dispersions in D₂O revealed that within the aggregates' hydrophobic domains, individual molecules are accessible to the solvent, as evidenced by the sharp hydrocarbon peaks (Figure 4a), which are similar to those of polysorbate 20 micelles (Figure 4b). However, the ¹H NMR spectra of the sorbitan monostearate (Figure 4c) and 12G0 vesicles (Figure 3c, Figure 4d) reveal that the hydrophobic domains in these vesicles are less accessible to the solvent as evidenced by the broad hydrocarbon peaks. The broad hydrocarbon peak shows that the aqueous solvent has limited access to the sorbitan monostearate and 12G0 hydrophobic domains and that both sorbitan monostearate and 12G0 aggregates produce more apolar domains than those produced by the micellar polysorbate dispersions and particulate 12G1 dispersions.

Additionally the signal for water was narrow in the case of polysorbate 20 but comparatively broader in the case of 12G1 aggregates, sorbitan monostearate vesicles and 12G0 vesicles. Broad NMR signals indicate that the atoms are in a variety of

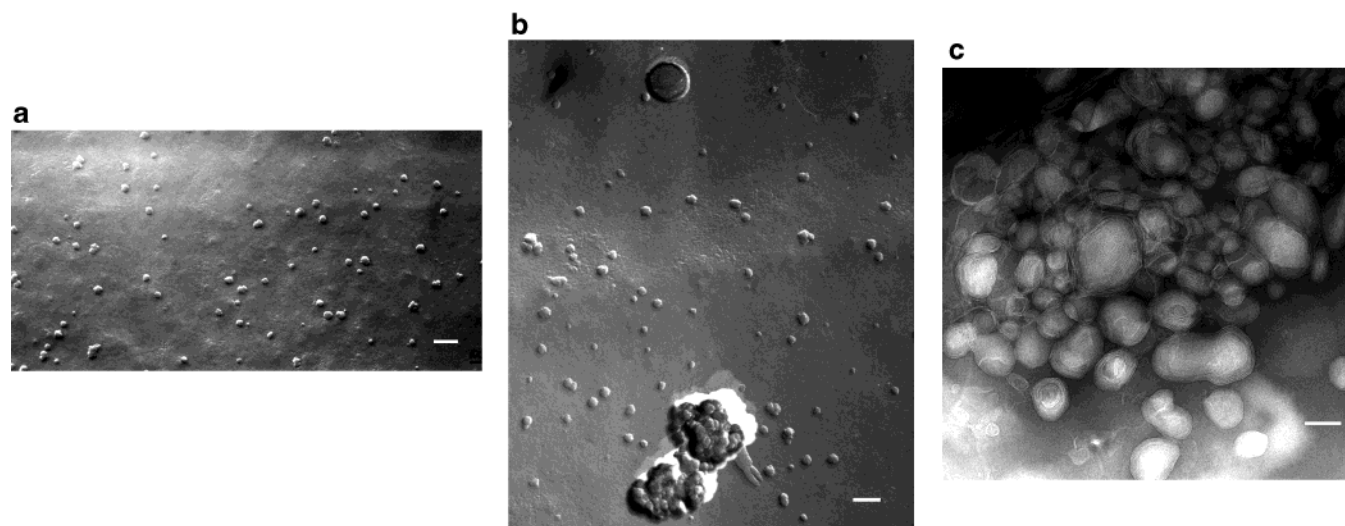


Figure 3. (a) Freeze fracture electron micrograph of 12G1 aggregates (2.6 mM), bar = 100 nm. (b) Freeze fracture electron micrograph of 12G1 aggregates (35 mM), bar = 100 nm. (c) Negative stained transmission electron micrograph of 12G0, cholesterol (21 mM:21 mM) vesicles, bar = 100 nm.

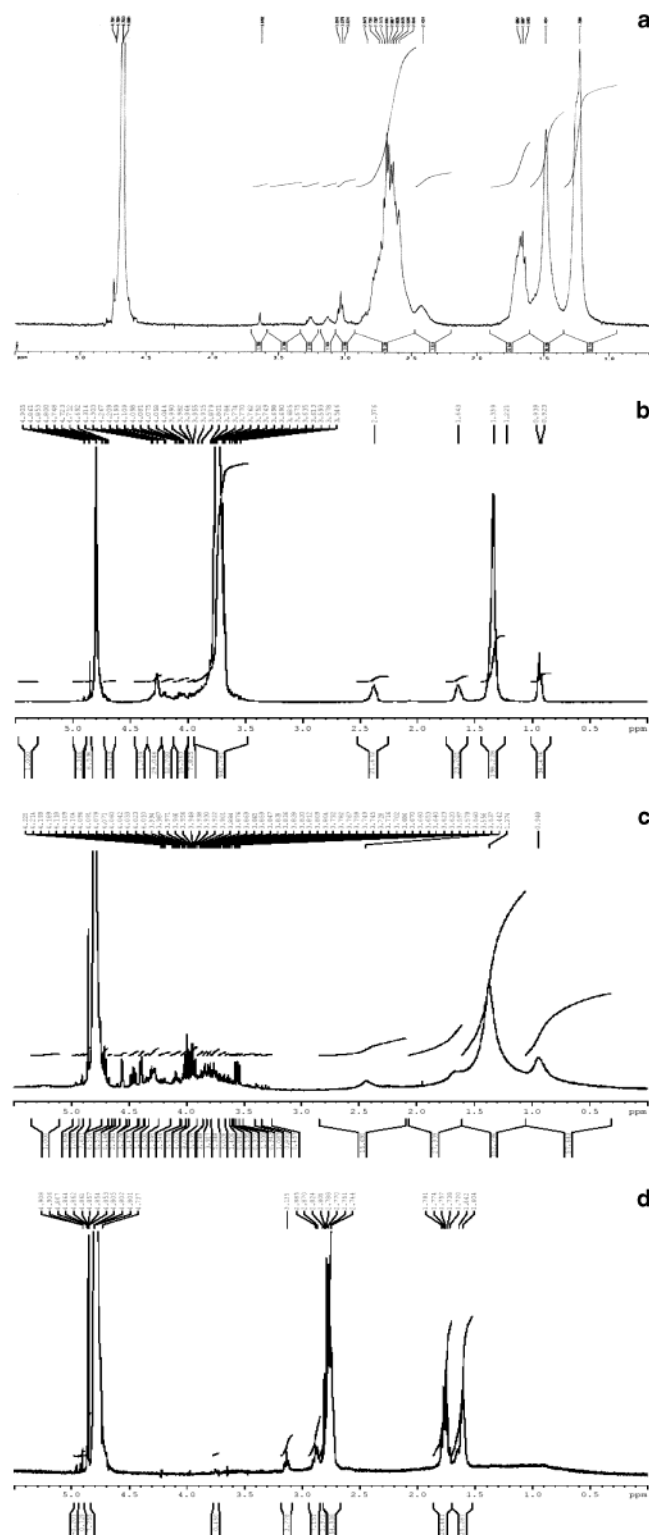


Figure 4. (a) ^1H NMR spectrum of 12G1 aggregates in D_2O (14 mM, 8 mg mL^{-1}). (b) ^1H NMR spectrum of polysorbate 20 in D_2O (8 mg mL^{-1}). (c) ^1H NMR spectrum of sorbitan monostearate vesicles in D_2O (14 mM, 8 mg mL^{-1}). (d) ^1H NMR spectrum of 12G0, cholesterol (21 mM:21 mM – 8 mg mL^{-1} ; 8 mg mL^{-1}) vesicles in D_2O .

environments, and while in the case of the polysorbate 20 micelles the micelle interior will be largely inaccessible to water, water would reside within the 12G0 vesicles (Figure 3c) and sorbitan monostearate vesicles.²⁶ The broad water peaks in the sorbitan monostearate and 12G0 vesicle– D_2O spectra indicate that water gains access to the interior of the structures. From the data in Figure 4, we can thus conclude that water is contained

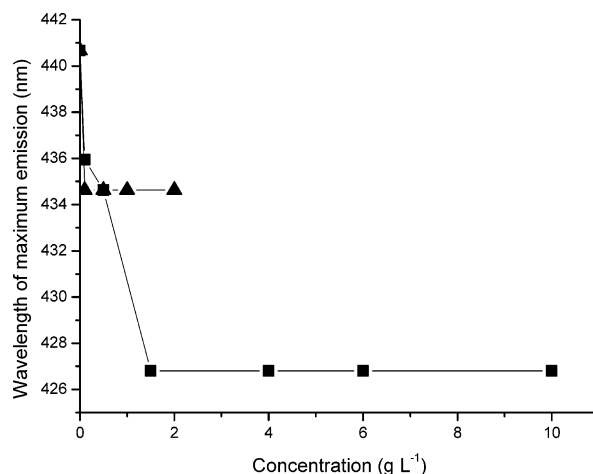


Figure 5. Wavelength of maximum fluorescence emission of TNS in the presence of various amphiphile dispersions ■ = 12G1, ▲ = sorbitan monostearate.

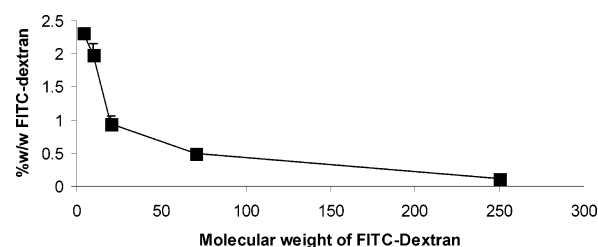


Figure 6. The encapsulation of FITC-dextran by 12G1. Initial Concentration of 12G1 = 14 mM and initial concentration of FITC-dextran = 10 mg mL^{-1} .

within the 12G1 aggregates, indicating that 12G1 aggregates are vesicular (with an aqueous core) and not micellar in nature.

Nanoviscosity of Hydrophobic Domains. The fluorescence emission spectra of TNS on incorporation into an area of low polarity and high viscosity is blue shifted and increases in intensity.²⁰ Figure 5 illustrates the blue shift encountered by the probe on incorporation within 12G1 aggregates and sorbitan monostearate niosomes, evidence that a change in the polarity/viscosity of the environment is perceived in these self-assembled systems. This shift is more pronounced with the 12G1 assemblies. As sorbitan monostearate has a C18 chain while 12G1 has a C12 chain, it is likely that the probe perceives a less viscous environment in the presence of 12G1 aggregates when compared to sorbitan monostearate vesicles and not a more hydrophobic environment. This can be explained by the presence of a high number of fused aggregates with higher concentrations of 12G1. It is suggested that these fused aggregates are the result of the bridging of particles by bolaamphiphiles in which the polar headgroups actually reside in two separate fused particles. This is the only explanation for the fusion of aggregates that is observed. The high area per molecule data obtained from the surface tension plots (73.4 \AA^2) provide evidence that the molecule may adopt a conformation whereby both ends of the molecule are in contact with a hydrophilic environment. Bridging amphiphiles will enjoy considerably less mobility than other membrane resident amphiphiles such as those resident in the sorbitan monostearate vesicles.

Analysis of Hydrophilic Domains. An investigation of the hydrophilic domains, evidenced by the ^1H NMR data (Figure 4), indicates that 12G1 is able to encapsulate the hydrophilic polymer fluorescein isothiocyanate dextran (Figure 6). The encapsulation efficiency of 12G1 for the 4kD molecular weight compound was $23.2 \pm 0.28 \text{ mg per g}$ of surfactant which was

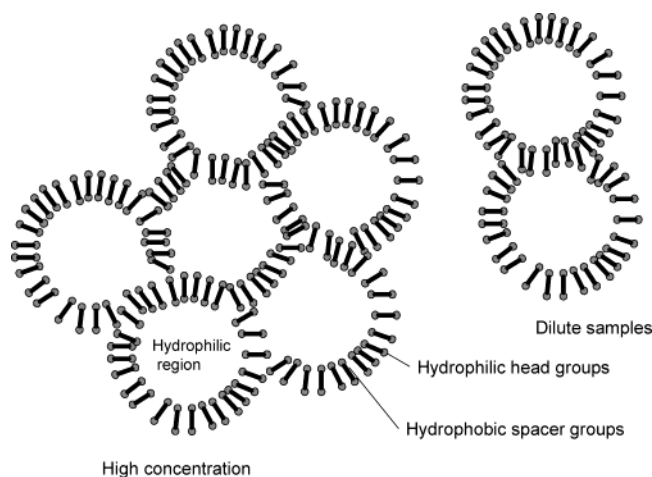


Figure 7. Schematic depiction of the arrangement of amphiphile molecules in 12G1 aggregates.

136X that obtained with sorbitan monostearate, cholesterol vesicles (0.17 ± 0.016 mg per g of surfactant — sorbitan monostearate) and 45X that obtained with sorbitan monostearate vesicles (0.51 ± 0.018 mg per g surfactant). These data are indicative of the high level of hydration experienced by these nanoparticle systems. As the molecular weight of the FITC-dextran molecule increases the encapsulation efficiency is diminished (Figure 6), indicating that the individual hydrophilic domains are of limited volume.

General Discussion

Galactose—spermine double-chain asymmetric bolaamphiphiles have been synthesized for gene delivery²⁷ and C6, C7, C8, and C10 amide dispermine bolaamphiphiles have been synthesized as inhibitors of spermidine transport in breast cancer cells.²⁸ Spermine bolaamphiphiles may thus have important biomedical applications yet their self-assembly has not been studied. While the C8 and C10 alkyl spermine bolaamphiphiles of the current report did not self-assemble in aqueous media (Figure 2b), the C12 compound self-assembled into particulate structures of 20 nm in diameter which gave isotropic liquids at low concentration.

We must turn our attention to the nature of the spherical aggregates observed in the transmission electron micrographs. First of all these particles show no sign of being individually fractured as only convex fracture faces are seen (Figure 3a). Monolayer membranes prepared from membrane spanning lipids usually show a series of concentric circles across the fracture plane due to the presence of the membrane spanning lipids which leads to cross-fracturing.¹⁴ The present individual particles appear too small to be fractured or resist fracturing due to the presence of fusion faces. We further assert that these particles are nonbilayer in nature especially as U-shaped conformations are difficult for small hydrophobic spacer bolaamphiphiles to attain.^{5,25} It was also not possible to visualize the monolayer using transmission electron microscopy (data not shown). Monolayer membranes are by their very nature thinner¹ than conventional bilayer membranes and thus would be more difficult to visualize. However, the FITC-dextran encapsulation (Figure 6), D₂O ¹H NMR (Figure 4) and freeze fracture electron microscopy (Figure 3a&b) data point to 12G1 aggregates being fused monolayer membrane vesicles with a sponge like structure as schematically shown in Figure 7. Monolayer membrane vesicles were thought not to fuse because of the inability of the charged headgroup to cross the hydrophobic membrane and form

bridges.¹ However in the case of 12G1, the hydrophilic headgroup is relatively nonpolar (spermine dissolves appreciably in ethanol and chloroform as well as water) and is thus able to form bridges between particles. With higher 12G1 concentrations, particles fuse to a greater degree to give larger aggregates of the smaller 20 nm aggregates, and these latter larger species have a very high hydrophilic loading capacity (Figure 6). Transparent 60–200 nm nanoparticles have been reported with a C12 crown ether bolaamphiphile which were observed to grow in neutral or slightly alkaline pH and at 35 °C,⁹ while the fusion of 100 nm aggregates prepared from carboxylic acid bolaamphiphiles has been observed at acid and neutral pH.⁷ What is clear is that a lowering of the hydration of these aggregates by either diminishing ionization as in the case of the carboxylic acid bolaamphiphiles,⁷ diminishing hydrogen bonding in the case of the crown ether bolaamphiphiles⁹ or increasing concentration as seen here, leads to the appearance of fused and larger aggregates. With 12G1, a diminished hydration of the headgroup allows bridging by reducing the energy associated with movement of the bridging molecules through the monolayer membrane. Further evidence of the involvement of individual molecules in the bridging of fused vesicles is found in the fact that the hydrocarbon portion of the molecule resides within a relatively viscous environment (Figure 5). The viscous hydrophobic environment stems from the bridging events between the particles (Figure 3, Figure 7). The evidence that the image in Figure 3b represents a number of fused smaller vesicles is found in the fact that the hydrophilic domains are abundant but of a finite and relatively small size (Figure 6).

It is possible that structures similar to ours have been prepared previously but not described, since “loose well hydrated” non micellar particles have been reported for C12 diquaternary ammonium bolaamphiphiles⁸ and transparent 60–200 nm nanoparticles have been observed with a C12 crown ether bolaamphiphile.⁹ The latter nanoparticles were observed to grow in neutral or slightly alkaline pH at a temperature of 35 °C.

The model presented in Figure 7 best encapsulates all the evidence and we thus present a new type of assembly from bolaamphiphiles. The amphiphiles assemble into a series of fused particles leading to a sponge type structure made up of individual monolayer vesicles. However, within the fused materials there are abundant hydrophilic pockets for the residence of hydrophilic solutes. The size of the individual aggregates (20 nm) would be in keeping with such a structure. However, rarely are individual monolayer vesicular structures seen due to the bridging of each single particle by individual molecules to form dimers and trimers even at low bolaamphiphile concentrations (Figure 3a and Figure 7). When compared to the C8 and C10 bolaamphiphiles, the C12 bolaamphiphile has a sufficient degree of hydrophobicity to allow for monomer aggregation. The single-headed surfactant 12G0 is understandably more hydrophobic than 12G1 and also unable to form the bridged structures and hence forms conventional bilayer vesicles.

References and Notes

- (1) Fuhrhop, J.-H.; Fritsch, D. *Acc. Chem. Res.* **1986**, *19*, 130–137.
- (2) Fuhrhop, J.-H.; Spiroski, D.; Boettcher, C. *J. Am. Chem. Soc.* **1993**, *115*, 1600–1601.
- (3) Kosigo, M.; Ohnishi, S.; Yase, K.; Masuda, M.; Shimzu, T. *Langmuir* **1998**, *14*, 4978–4986.
- (4) Kosigo, M.; Hanada, T.; Yase, K.; Shimzu, T. *Chem. Commun.* **1988**, 1791–1792.
- (5) Franceschi, S.; Andreu, V.; Viguerie, N.d.; Riviere, M.; Lattes, A.; Moisan, A. *New J. Chem.* **1998**, 225–231.

- (6) Meglio, C. D.; Ravanavare, S.; Svenson, S.; Thompson, D. H. *Langmuir* **2000**, *16*, 128–133.
- (7) Fuhrhop, J.-H.; David, H.-H.; Mathieu, J.; Liman, U.; Winter, H. J.; Boekema, E. J. *J. Am. Chem. Soc.* **1986**, *108*, 1785–1791.
- (8) Yiv, S.; Kale, K. M.; Lang, J.; Zana, R. *J. Phys. Chem.* **1976**, *80*, 2651–2655.
- (9) Munoz, S.; Mallen, J. V.; Nakano, A.; Chen, Z. H.; Gay, I.; Echegoyen, L.; Gokel, G. W. *J. Chem. Soc.-Chem. Commun.* **1992**, 520–522.
- (10) Prata, C.; Mora, N.; Polidori, A.; Lacombe, J. M.; Pucci, B. *Carbohydr. Res.* **1999**, *321*, 15–23.
- (11) Davey, T. W.; Ducker, W. A.; Hayman, A. R. *Langmuir* **2000**, *16*, 2430–2435.
- (12) Liu, M.; Cai, J. *Langmuir* **2000**, *16*, 2899–2901.
- (13) Rivaux, Y.; Noiret, N.; Patin, H. *New J. Chem* **1998**, 857–863.
- (14) Guilbot, J.; Benvegnu, T.; Legros, N.; Plusquellec, D. *Langmuir* **2001**, *17*, 613–619.
- (15) Fuhrhop, J.-H.; Tank, H. *Chem. Phys. Lipids* **1987**, *43*, 193–213.
- (16) Bosch, M. P.; Parra, J. L.; Sanchezbaeza, F. *Can. J. Chem.-Rev. Can. Chim.* **1993**, *71*, 2095–2101.
- (17) Kalyanasundaram, K.; Thomas, J. K. *J. Am. Chem. Soc.* **1977**, *99*, 2039–2044.
- (18) Lieske, A.; Jaeger, W. *Tens. Surfact. Deterg.* **1999**, *36*, 155–161.
- (19) Han, S. O.; Mahato, R. I.; Kim, S. W. *Bioconjugate Chem.* **2001**, *12*, 337–345.
- (20) Nakashima, K.; Takeuchi, K. *Appl. Spectrosc.* **2001**, *55*, 1237–1244.
- (21) Uchegbu, I. F.; Florence, A. T. *Adv. Coll. Interface Sci.* **1995**, *58*, 1–55.
- (22) Yoshioka, T.; Sternberg, B.; Florence, A. T. *Int. J. Pharm.* **1994**, *105*, 1–6.
- (23) Han, S. O.; Mahato, R. I.; Kim, S. W. *Bioconjugate Chem.* **2001**, *12*, 337–345.
- (24) Rivaux, Y.; Noiret, N.; Patin, H. *New J. Chem.* **1998**, *22*, 857–863.
- (25) Menger, F. M.; Wrenn, S. J. *J. Phys. Chem.* **1974**, *78*, 1387–1390.
- (26) Uchegbu, I. F.; Double, J. A.; Turton, J. A.; Florence, A. T. *Pharmaceut. Res.* **1995**, *12*, 1019–24.
- (27) Gaucheron, J.; Santaella, C.; Vierling, P. *Bioconjugate Chem.* **2001**, *12*, 569–575.
- (28) Graminski, G. F.; Carlson, L.; Ziemer, J. R.; Cai, F.; Vermeulen, N. M. J.; Vanderwerf, S. M.; Burns, M. R. *Biog. Med. Chem. Lett.* **2002**, *12*, 35–40.